

Rochester Institute of Technology

RIT Digital Institutional Repository

Articles

Faculty & Staff Scholarship

4-15-2009

Algebraic Classification of Numerical Spacetimes and Black-Hole-Binary Remnants

Manuela Campanelli

Rochester Institute of Technology

Carlos O. Lousto

Rochester Institute of Technology

Yosef Zlochower

Rochester Institute of Technology

Follow this and additional works at: <https://repository.rit.edu/article>

Recommended Citation

M. Campanelli, C. Lousto, Y. Zlochower, Phys. Rev. D 79, 084012 (2009). <https://doi.org/10.1103/PhysRevD.79.084012>

This Article is brought to you for free and open access by the RIT Libraries. For more information, please contact repository@rit.edu.

Algebraic Classification of Numerical Spacetimes and Black-Hole-Binary Remnants

Manuela Campanelli, Carlos O. Lousto, and Yosef Zlochower

*Center for Computational Relativity and Gravitation, and
School of Mathematical Sciences, Rochester Institute of Technology,
78 Lomb Memorial Drive, Rochester, New York 14623*

(Dated: November 18, 2008)

In this paper we develop a technique for determining the algebraic classification of a numerical spacetime, possibly resulting from a generic black-hole-binary merger, using the Newman-Penrose Weyl scalars. We demonstrate these techniques for a test case involving a close binary with arbitrarily oriented spins and unequal masses. We find that, post merger, the spacetime quickly approaches Petrov type II, and only approaches type D on much longer timescales. These techniques allow us to begin to explore the validity of the “no-hair theorem” for generic merging-black-hole spacetimes.

PACS numbers: 04.25.Dm, 04.25.Nx, 04.30.Db, 04.70.Bw

I. INTRODUCTION

The recent breakthroughs in numerical relativity [1, 2, 3] that allowed for stable evolutions of black-hole-binary spacetimes led to many advancements in our understanding of black-hole physics, and it is now possible to accurately simulate the merger process and examine its effects in this highly non-linear regime [4, 5, 6, 7, 8, 9, 10, 11, 12, 13, 14, 15, 16, 17, 18]. Black-hole binaries radiate between 2% and 8% of their total mass and up to 40% of their angular momenta in the last few orbits, depending on the magnitude and direction of the spin components, during the merger [4, 5, 6] (ultra-relativistic head-on black-hole mergers can radiate up to $\sim 14\%$ of their mass [19]). In addition, the radiation of net linear momentum by a black-hole binary leads to the recoil of the final remnant hole [20, 21, 22, 23, 24, 25, 26, 27, 28, 29, 30, 31, 32, 33, 34, 35, 36, 37, 38, 39, 40, 41, 42, 43], which can have astrophysically observable important effects [20, 42, 44, 45, 46, 47, 48, 49, 50, 51, 52, 53] and represents the first strong-field test of General Relativity (GR).

In addition to important astrophysical applications, the two body problem in GR is intrinsically interesting because it provides the framework for analyzing the behavior of the theory in the highly-nonlinear, highly-dynamical, non-symmetrical regime. For example, the cosmic censorship hypothesis, that states that singularities in the universe should be cloaked by a horizon is under active investigation [4, 5, 6, 54, 55]. In this paper we are interested in verifying the “no hair theorem”, that states that the final state of a black hole, for instance as the byproduct of a multi-black-hole mergers [56, 57], is a Kerr black hole [58].

The problem of determining the geometry of the final stage of a black-hole binary merger arises as a practical question even in perturbative techniques, such as the Lazarus approach [59, 60], which used a combined numerical and perturbative approach to simulate the waveforms from a binary merger. In the context of the Lazarus approach, it is crucial to determine when the transi-

tion from numerical to perturbative evolutions is possible, i.e. when the full numerical simulation could be approximated by (relatively small) perturbations of a Kerr-rotating black hole, and a diagnostic, the S-invariant [61]

$$S = 27J^2/I^3, \quad (1)$$

that is identically 1 for a Kerr spacetime, was developed to measure the closeness of the spacetime to an algebraically special type II. However, the S-invariant by itself is not sufficient to demonstrate that the spacetime is near Kerr because it does not distinguish between type II and type D spacetimes.

More recently, with the availability of new long term evolutions, one of the consistency tests performed is the agreement of the total angular momentum of the system when computed in three different ways: by measuring the angular momentum (and mass) of the remnant black hole [5, 6, 22] using the isolated horizon formulae [62], by measuring the total energy and angular momentum radiated [63, 64] and subtracting it from the total initial values, and by looking at the quasi-normal frequencies of the late-time waveforms and associate them with those of a rotating Kerr hole with mass M and angular momentum per mass a [23]. The rough agreement of those values represents weak evidence that the final black hole is of the Kerr type.

No hair theorems assume a stationary Killing vector [58] as characterizations of the Kerr geometry [65, 66]. While one can classify spacetimes based on their symmetry properties, here we will use a classification method based on the algebraic properties of generic spacetimes without a-priori assumptions about symmetries.

Demonstrating that the remnant of a black-hole merger approaches Kerr asymptotically (in time) would also help answer open questions about the stability of Kerr under arbitrary perturbations. The stability of the Kerr spacetime under linear perturbations has only been proven mode-by-mode [67], and the interior of the hole may even be unstable [68]. Hence a study of the invariant geometrical properties of the black-hole merger, which would yield a highly-nontrivial perturbation of the

‘Kerr’ background, may answer many open questions.

II. MATHEMATICAL TECHNIQUES

A. Petrov type

The Petrov classification of a generic spacetime is related to the number of distinct principle null directions (PND) of the Weyl tensor. A generic spacetime will have four linearly independent null vectors k^μ (i.e. PNDs) at all points that satisfy

$$k^\nu k^\rho k_{[\tau} C_{\mu]\nu\rho[\sigma} k_{\chi]}. \quad (2)$$

Type I spacetimes have four distinct PNDs, Type II have three distinct PNDs (1 pair and two additional distinct PNDs), Type III have two distinct PNDs with one PND of multiplicity three, Type D spacetimes have two distinct PNDs consisting of two pairs of PNDs of multiplicity two, type N spacetimes have a single PND of multiplicity four, and Type O spacetimes have $C_{\mu\nu\rho\sigma} = 0$.

If the tetrad is chosen such that l^a is a PND, then the Weyl scalar $\psi_0 = C_{\mu\nu\rho\sigma} l^\mu m^\nu l^\rho m^\sigma$ vanishes, and similarly, if $\psi_0 = 0$, then l^a is a PND. Hence the algebraic classification of the spacetime can be obtained by finding the number of distinct choices of l^a for which $\psi_0 = 0$. This amounts to finding the roots (and multiplicity of the roots) of the quartic equation (See Ref. [69], Eq. (9.5))

$$\psi_0 + 4\lambda\psi_1 + 6\lambda^2\psi_2 + 4\lambda^3\psi_3 + \lambda^4\psi_4 = 0, \quad (3)$$

where ψ_0, \dots, ψ_4 are the Weyl scalars in an arbitrary tetrad, restricted only by the condition $\psi_4 \neq 0$. This is equivalent to finding a tetrad rotation such that $\psi_0 = 0$, and if the root is repeated, then in this tetrad, $\psi_1 = 0$ (similarly if the multiplicity of the root is 3 or 4 then $\psi_2 = 0$ and $\psi_3 = 0$ respectively). If, as in type D spacetimes, there are two pairs of repeated PNDs, then we can choose a tetrad where the only non-vanishing Weyl scalar is ψ_2 . It is important to note that the algebraic classification is done pointwise. A spacetime, as a whole, is of a particular type, if at every point the algebraic classification is of that type.

In order to determine if the numerical spacetime is algebraically special (within the numerical errors) we follow [70] and [69], Ch. 4. We start by defining the scalar invariants [71]

$$I = \frac{1}{2} \tilde{C}_{abcd} \tilde{C}^{abcd} \quad \text{and} \quad J = -\frac{1}{6} \tilde{C}_{abcd} \tilde{C}^{cd}_{mn} \tilde{C}^{mnab}. \quad (4)$$

where $\tilde{C}_{abcd} = \frac{1}{4}(C_{abcd} + \frac{i}{2}\epsilon_{abmn} C^{mn}_{cd})$ (i.e. 1/2 the conjugate of the self-dual part of the Weyl tensor C_{abcd}).

If a spacetime has repeated principal null directions it is algebraically special. If this is the case, Eq. (3) has at least two repeated roots. In any case, Eq. (3) can be transformed into a depressed quartic (see Eq. (9) below)

that, in turn, can be converted into a depressed nested cubic with roots y , which satisfy the condition

$$y^3 - Iy + 2J = 0. \quad (5)$$

Algebraic specialty then implies

$$I^3 = 27J^2, \quad (6)$$

i.e. $S = 1$ in Eq. 1. For Types *II* and *D* the invariants I and J are non-trivial, while for Types *III*, *N*, and *O* they vanish identically.

For practical applications, it is convenient to write the invariants in terms of Weyl scalars in an arbitrary null tetrad

$$I = 3\psi_2^2 - 4\psi_1\psi_3 + \psi_4\psi_0, \quad (7)$$

$$J = -\psi_2^3 + \psi_0\psi_4\psi_2 + 2\psi_1\psi_3\psi_2 - \psi_4\psi_1^2 - \psi_0\psi_3^2. \quad (8)$$

In order to completely determine the algebraic type we reduce Eq. (3), by changing to the variable $x = \lambda\psi_4 + \psi_3$ [72], to the form

$$x^4 + 6Lx^2 + 4Kx + N = 0, \quad (9)$$

where

$$K = \psi_1\psi_4^2 - 3\psi_4\psi_3\psi_2 + 2\psi_3^3, \quad (10)$$

$$L = \psi_2\psi_4 - \psi_3^2, \quad (11)$$

$$N = \psi_4^2 I - 3L^2 \\ = \psi_4^3 \psi_0 - 4\psi_4^2 \psi_1 \psi_3 + 6\psi_4 \psi_2 \psi_3^2 - 3\psi_3^4 \quad (12)$$

(note the typo in the definition of N in Refs. [69, 70]). For a type *II* spacetime, $K \neq 0$ and $N - 9L^2 \neq 0$, while for type *D* and *III* spacetimes, $K = 0$ and $N - 9L^2 = 0$ with $N \neq 0$. For a type *N* spacetime, $K = 0$ and $L = 0$ (hence $N = 0$).

Note that the above scalar objects are not invariant under arbitrary tetrad rotations (See Ref. [73], Chapter 1, Eqs. (342), [note typo there], (346) and (347)). In particular they transform as

$$\begin{aligned} L &\rightarrow A^2 e^{-2i\theta} L, \\ K &\rightarrow A^3 e^{-3i\theta} K, \\ N &\rightarrow A^4 e^{-4i\theta} N. \end{aligned} \quad (13)$$

for Type III rotations and

$$\begin{aligned} L &\rightarrow L, \\ K &\rightarrow K, \\ N &\rightarrow N, \end{aligned} \quad (14)$$

for Type II rotations. Similar expressions for Type I rotations do not have these simple forms, but we verified that, if as in type D solutions, $K = 0$ and $N - 9L^2 = 0$ in the original tetrad, then $K = 0$ and $N - 9L^2 = 0$ in the new rotated tetrad (this is also obvious for type III and II transformations above). One the other hand $L = 0$ is not preserved by type I rotations.

Coming back to the roots x_1, x_2, x_3, x_4 of the Eq. (9), we observe that, in numerically generated spacetimes, the roots never agree exactly, even if the metric is expected to be of a special algebraic type. Of course, the root differences in each pair should scale with resolution and asymptotically approach zero as $h \rightarrow 0$ and $t \rightarrow \infty$.

The roots of Eq. (3) can be obtained from the roots of Eq. (5)i using the following algorithm [74]

$$\begin{aligned} D &= J^2 - (I/3)^3, \\ A &= (-J + \sqrt{D})^{1/3}, \quad B = (-J - \sqrt{D})^{1/3}, \\ y_1 &= A + B, \\ y_2 &= -\frac{1}{2}(A + B) + i\frac{\sqrt{3}}{2}(A - B), \\ y_3 &= -\frac{1}{2}(A + B) - i\frac{\sqrt{3}}{2}(A - B), \end{aligned} \quad (15)$$

where the complex phases of A and B are chosen such that $AB = I/3$. The roots of Eq. (9) are then obtained from the roots of the complete cubic equation for the variable z (where $z = 2\psi_4 y - 4L$)

$$z^3 + 12Lz^2 + 4(9L^2 - N)z - 16K = 0, \quad (16)$$

which has the roots

$$\begin{aligned} z_1 &= 2\psi_4 y_1 - 4L, \\ z_2 &= 2\psi_4 y_2 - 4L, \\ z_3 &= 2\psi_4 y_3 - 4L. \end{aligned} \quad (17)$$

Finally the roots of our original equation (3) can be written in the form [72]

$$\begin{aligned} \lambda_1 &= \left[-\psi_3 + \frac{1}{2}(\sqrt{z_1} + \sqrt{z_2} + \sqrt{z_3}) \right] / \psi_4, \\ \lambda_2 &= \left[-\psi_3 + \frac{1}{2}(\sqrt{z_1} - \sqrt{z_2} - \sqrt{z_3}) \right] / \psi_4, \\ \lambda_3 &= \left[-\psi_3 + \frac{1}{2}(-\sqrt{z_1} + \sqrt{z_2} - \sqrt{z_3}) \right] / \psi_4, \\ \lambda_4 &= \left[-\psi_3 + \frac{1}{2}(-\sqrt{z_1} - \sqrt{z_2} + \sqrt{z_3}) \right] / \psi_4, \end{aligned} \quad (18)$$

where the signs of the $\sqrt{z_i}$ are chosen such that $(\sqrt{z_1}\sqrt{z_2}\sqrt{z_3}) = -4K$. We note that in a type D spacetime $\lambda_1 = \lambda_2$ and $\lambda_3 = \lambda_4$.

B. Vacuum

The determination of the algebraic type of the matter fields can be done in an analogous way using the Ricci tensor, rather than the Weyl scalars. The analogue of the Petrov types are the Segre types and the equation to determine the multiplicities of the roots is ([69], Eq. (9.2))

$$\sigma^4 - \frac{1}{2}I_6\sigma^2 - \frac{1}{3}I_7\sigma + \frac{1}{8}(I_6^2 - 2I_8) = 0, \quad (19)$$

where

$$I_6 = S_b^a S_a^b, \quad (20)$$

$$I_7 = S_b^a S_c^b S_a^c, \quad (21)$$

$$I_8 = S_b^a S_c^b S_d^c S_a^d, \quad (22)$$

and

$$S_{ab} = R_{ab} - \frac{1}{4}g_{ab}R, \quad (23)$$

is the trace free part of the Ricci tensor.

This characterization of the matter fields does not completely determine the algebraic properties, and other additional criteria have to be used. In our numerical simulations here, we are concerned with vacuum spacetimes. Numerical evolutions may introduce artificial (and unphysical) matter fields through violations of the Hamiltonian and momentum constraints, and the natural way of monitoring the accuracy of the solution is to examine these constraints and confirm that the induced matter fields converge to zero.

C. Determination of the Kerr solution

Once we determine that a solution is, for instance, Petrov type D and is a vacuum solution, we still do not uniquely single out the Kerr spacetime. One can go further and try to determine if the spacetime has the symmetries of Kerr (the Kerr spacetime has two commuting spacelike and timelike Killing vectors [75]). However, one still needs to examine the asymptotic behavior of the solutions to determine that the spacetime does not have a NUT charge.

A general type D, vacuum solution can be described by the metric ([69], Eq. (21.17)),

$$\begin{aligned} ds^2 &= (p^2 + r^2)(d\theta^2 + dr^2/Y) \\ &\quad + a^2 \sin^2 \theta (d\tau + r^2 d\sigma)^2 / (p^2 + r^2) \\ &\quad - Y(d\tau - p^2 d\sigma)^2 / (p^2 + r^2), \end{aligned} \quad (24)$$

where $p = l - a \cos \theta$, $\sigma = -\varphi/a$, $\tau = t + a\varphi$, $Y = a^2 - l^2 - 2mr + r^2$, m is the mass, a is the specific spin, and l the NUT parameter of the black hole. If the null tetrad is aligned with the principal null directions, i.e.

$$l^\mu, n^\mu = (r^2 \partial_\tau - \partial_\sigma) / Y \pm \partial_r, \quad (25)$$

then the only non-vanishing Weyl scalar is

$$\psi_2 = -(m + il)(r + i(l - a \cos \theta))^{-3}. \quad (26)$$

It is then natural to look at the asymptotic behavior of the spacetime to determine if there is a NUT charge l , or if the spacetime is Kerr. One can use the method of determining a quasi-Kinnersley frame [59, 76] to compute ψ_2 and perform the above analysis. Alternatively, we can use the fact that, once we determined the spacetime is

type D, we can choose a tetrad where all the Weyl scalars, but ψ_2 , vanish. Hence the invariants I and J must have the form

$$I = 3\psi_2^2, \quad J = -\psi_2^3 \quad (27)$$

in this special class of tetrads.

An asymptotic expansion of the I invariant for the metric (24) then gives

$$I = \frac{3}{r^6}(m + il)^2 - \frac{18i}{r^7}(m + il)^2(l - a \cos \theta) + \mathcal{O}\left(\frac{1}{r^8}\right), \quad (28)$$

and, by looking at the real and imaginary parts of the I invariant at large radii, we can determine the l parameter via

$$\Im(I)/\Re(I) = \begin{cases} \frac{2ml}{m^2 - l^2}; & l \neq 0, \\ \frac{6a \cos \theta}{r}; & l = 0. \end{cases} \quad (29)$$

We will use this method to determine the asymptotic behavior of the final remnant of a black-hole-binary merger. Note that using I and J only requires smooth second derivatives of the metric, which has a distinct advantage over higher-derivative methods when dealing with numerically generated spacetimes.

III. NUMERICAL TECHNIQUES

To compute the numerical initial data, we use the puncture approach [77] along with the `TWOPUNCTURES` [78] code. In this approach the 3-metric on the initial slice has the form $\gamma_{ab} = (\psi_{BL} + u)^4 \delta_{ab}$, where ψ_{BL} is the Brill-Lindquist conformal factor, δ_{ab} is the Euclidean metric, and u is (at least) C^2 on the punctures. The Brill-Lindquist conformal factor is given by $\psi_{BL} = 1 + \sum_{i=1}^n m_i^p / (2|\vec{r} - \vec{r}_i|)$, where n is the total number of ‘punctures’, m_i^p is the mass parameter of puncture i (m_i^p is *not* the horizon mass associated with puncture i), and \vec{r}_i is the coordinate location of puncture i . We evolve these black-hole-binary data-sets using the `LAZEV` [79] implementation of the moving puncture approach [2, 3]. In our version of the moving puncture approach we replace the BSSN [80, 81, 82] conformal exponent ϕ , which has logarithmic singularities at the punctures, with the initially C^4 field $\chi = \exp(-4\phi)$. This new variable, along with the other BSSN variables, will remain finite provided that one uses a suitable choice for the gauge. An alternative approach uses standard finite differencing of ϕ [3]. Recently Marronetti *et al.* [83] proposed the use of $W = \sqrt{\chi}$ as an evolution variable. For the runs presented here we use centered, eighth-order finite differencing in space [56] and fourth-order Runge-Kutta time integrator (note that we do not upwind the advection terms).

We use the Carpet [84] mesh refinement driver to provide a ‘moving boxes’ style mesh refinement. In this approach refined grids of fixed size are arranged about the coordinate centers of both holes. The Carpet code then

moves these fine grids about the computational domain by following the trajectories of the two black holes.

We obtain accurate, convergent waveforms and horizon parameters by evolving this system in conjunction with a modified 1+log lapse and a modified Gamma-driver shift condition [2, 85], and an initial lapse $\alpha(t = 0) = 2/(1 + \psi_{BL}^4)$. The lapse and shift are evolved with

$$(\partial_t - \beta^i \partial_i) \alpha = -2\alpha K, \quad (30a)$$

$$\partial_t \beta^a = B^a, \quad (30b)$$

$$\partial_t B^a = 3/4 \partial_t \tilde{\Gamma}^a - \eta B^a. \quad (30c)$$

These gauge conditions require careful treatment of χ , the inverse of the three-metric conformal factor, near the puncture in order for the system to remain stable [2, 7, 8]. As shown in Ref. [86], this choice of gauge leads to a strongly hyperbolic evolution system provided that the shift does not become too large. In our tests, W showed better behavior at very early times ($t < 10M$) (i.e. did not require any special treatment near the punctures), but led to evolutions with lower effective resolution when compared to χ .

We use `AHFINDERDIRECT` [87] to locate apparent horizons. We measure the magnitude of the horizon spin using the Isolated Horizon algorithm detailed in [62]. This algorithm is based on finding an approximate rotational Killing vector (i.e. an approximate rotational symmetry) on the horizon φ^a . Given this approximate Killing vector φ^a , the spin magnitude is

$$S_{[\varphi]} = \frac{1}{8\pi} \oint_{AH} (\varphi^a R^b K_{ab}) d^2V, \quad (31)$$

where K_{ab} is the extrinsic curvature of the 3D-slice, d^2V is the natural volume element intrinsic to the horizon, and R^a is the outward pointing unit vector normal to the horizon on the 3D-slice. We measure the direction of the spin by finding the coordinate line joining the poles of this Killing vector field using the technique introduced in [6]. Our algorithm for finding the poles of the Killing vector field has an accuracy of $\sim 2^\circ$ (see [6] for details). Note that once we have the horizon spin, we can calculate the horizon mass via the Christodoulou formula

$$m^H = \sqrt{m_{\text{irr}}^2 + S^2/(4m_{\text{irr}}^2)}, \quad (32)$$

where $m_{\text{irr}} = \sqrt{A/(16\pi)}$ and A is the surface area of the horizon.

We also use an alternative quasi-local measurement of the spin and linear momentum of the individual black holes in the binary that is based on the coordinate rotation and translation vectors [22]. In this approach the spin components of the horizon are given by

$$S_{[i]} = \frac{1}{8\pi} \oint_{AH} \phi_{[i]}^a R^b K_{ab} d^2V, \quad (33)$$

where $\phi_{[i]}^a = \delta_{\ell j} \delta_{mk} r^m \epsilon^{ijk}$, and $r^m = x^m - x_0^m$ is the coordinate displacement from the centroid of the hole,

while the linear momentum is given by

$$P_{[i]} = \frac{1}{8\pi} \oint_{AH} \xi_{[i]}^a R^b (K_{ab} - K\gamma_{ab}) d^2V, \quad (34)$$

where $\xi_{[\ell]}^i = \delta_\ell^i$.

A. Numerical Tetrad and Root Finder

We calculate $\psi_0 \cdots \psi_4$ using the tetrad

$$l^\mu = (t^\mu + r^\mu)/\sqrt{2}, \quad (35)$$

$$n^\mu = (t^\mu - r^\mu)/\sqrt{2}, \quad (36)$$

$$m^\mu = (\theta^\mu + i\phi^\mu)/\sqrt{2}, \quad (37)$$

where t^μ is the unit normal to the $t = \text{const}$ slices and $\{r^\mu, \theta^\mu, \phi^\mu\}$ are unit spacelike vectors (with time component equal to zero) constructed as follows [60]. We start with the unit vector

$$\phi^a = \widehat{\phi^a}, \quad (38)$$

where $\widehat{\phi^a} = \{-y, x, 0\}$, $\widehat{v^a} = v^a/\sqrt{v^a v^b \gamma_{ab}}$, and γ_{ab} is the spatial metric. We then find the unit vector in radial direction perpendicular to ϕ^a

$$r^a = \widehat{r^a}, \quad (39)$$

where

$$\widehat{r^a} = \check{r}^a - \check{r}^a \phi^b \gamma_{ab}, \quad (40)$$

and $\check{r}^a = \{x, y, z\}$. Finally, we obtain

$$\theta^a = \widehat{\theta^a}, \quad (41)$$

where

$$\widehat{\theta^a} = \gamma^{ab} \epsilon_{bcd} \phi^c r^d. \quad (42)$$

With this choice of tetrad $\psi_0 \cdots \psi_4$ are all non-vanishing for Kerr spacetimes when the specific spin a is non-vanishing.

In practice, we found that the roots of Eq. (3) are easily calculated using Newton's method. Here we start by assuming the root is $\lambda = 0$ and iterate until the root converges to order roundoff and obtain the root λ_1 . We then divide the polynomial by $(\lambda - \lambda_1)$ and repeat the procedure twice to find λ_2 and λ_3 . λ_4 is then obtained directly from the resulting first order polynomial. We then test that we found the true roots by comparing the polynomial $\psi_4 \Pi_{i=1}^4 (\lambda - \lambda_i)$ with the original polynomial (3). This procedure worked well because two of the roots in our case were always located near $\lambda = 0$. Thus we found that λ_1 and λ_2 always corresponded to the pair of roots near $\lambda = 0$. This procedure is repeated for all points in the spacetime that we analyzed.

TABLE I: Initial data parameters for the numerical evolution. The punctures have mass parameters m_i^p , horizons masses m_i^H , momenta $\pm \vec{p}$, spins \vec{S}_i , and the configuration has a total ADM mass $M_{\text{ADM}} = 1.0000004M$.

m_1^p/M	0.37752	m_2^p/M	0.42452
m_1^H/M	0.46298	m_2^H/M	0.57872
x_1/M	-0.75023	x_2/M	0.58004
y_1/M	1.11679	y_2/M	-0.89449
z_1/M	-0.16093	z_2/M	0.20338
S_1^x/M^2	-0.020765	S_2^x/M^2	0.12106
S_1^y/M^2	0.065806	S_2^y/M^2	-0.05532
S_1^z/M^2	0.054697	S_2^z/M^2	0.16178
p^x/M	-0.134735	p^y/M	-0.21376
p^z/M	-0.012323		

B. Initial Data

To generate the initial data parameters, we used random values for the mass ratio and spins of the binary (the ranges for these parameters were chosen to make the evolution practical). We then calculated approximate quasi-circular orbital parameters for a binary with these chosen parameters at an initial orbital separation of $50M$ and evolved using purely PN evolutions until the binary separation decreased to $2.3M$. The goal was to produce a binary that had no particular symmetries, so that we can draw general conclusions from the results, while also merging very quickly (within $15M$ of the start of the simulation), to reduce the computational expense. The initial binary configuration at $r = 50M$ was chosen such that $q = m_1/m_2 = 0.8$, $\vec{S}_1/m_1^2 = (-0.2, -0.14, 0.32)$, and $\vec{S}_2/m_2^2 = (-0.09, 0.48, 0.35)$. This is the same basic configuration that we used in [88]. We summarize the initial data parameters in Table I.

IV. RESULTS

We ran the binary configuration using 9 levels of refinement with an outer grid of resolution $h = 3.2M$ extending to ± 416 . The resolution on the finest grid was $h = M/80$. We analyze the Weyl scalars in the region $r \lesssim 5M$ where we had a resolution of $h \leq M/20$. This calculation is non-trivial because the magnitudes of the Weyl scalars can be quite small (we need to analyze these scalars at very late times when the waveform amplitudes are quite small), requiring very-high overall simulation accuracy. We found that the isolated horizon formulae and the radiated energy and angular momentum both predict similar remnant masses and spins, with the isolated horizon formulae Eqs. (31)-(33) giving $M_{\text{rem}} = 0.9859$, $\vec{S}_{\text{rem}} = \{0.00160 \pm 0.00005, 0.0407 \pm 0.0004, 0.7173 \pm 0.0001\}$ and the radiation giving $M_{\text{rem}} = 0.9861 \pm 0.0001$, $\vec{S}_{\text{rem}} = \{0.00153 \pm 0.00001, 0.04078 \pm 0.00002, 0.7179 \pm 0.0001\}$. A fit to the quasi-normal profile $\sim \exp(-\alpha t) \sin(\omega t)$ gives $\alpha = 0.07997 \pm 0.0013$ and $\omega = 0.5603 \pm 0.0025$, where

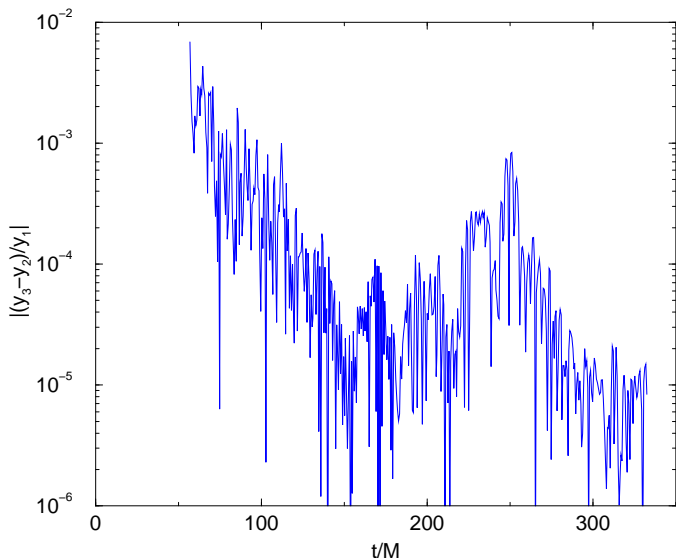


FIG. 1: The magnitude $|(y_3 - y_2)/y_1|$ versus time at the point $x = 5M, y = 0, z = 0$. The spacetime is algebraically special if $|(y_3 - y_2)/y_1| = 0$.

the values quoted are the average from fits to the real and imaginary parts of the $(\ell = 2, m = 2)$ component of ψ_4 extracted at $r = 100M$ over the domain $(160M < t < 200M)$. The resulting values of M_{rem} and a/M_{rem} [89] are 0.9876 ± 0.0079 and 0.743 ± 0.013 respectively. Note that the isolated horizon and radiated Energy/Momentum formulae predict that the final specific spin is $a/M_{\text{rem}} = 0.73931 \pm 0.00016$.

If the spacetime is algebraically special, then the roots y_2 and y_3 of Eq. (5) are equal. To measure how far the spacetime is from being algebraically special we plot the magnitude $|(y_3 - y_2)/y_1|$. In Fig. 1 we show this magnitude for the point $(x = 5M, y = z = 0)$ as a function of time. From the figure we can see that the deviation of the spacetime from being algebraically special decreases with time until $t \sim 150M$. The oscillation seen after this time may be due to reflections off of the refinement boundaries.

In Figs. 2-6 we show the magnitudes of the root-pair differences $|\lambda_1 - \lambda_2|$ and $|\lambda_3 - \lambda_4|$ both as a function of t at a fixed $(x, y, z) = (5, 0, 0)$ and along the x -axis at several times. Both pairs show a general decrease in the magnitudes of the differences with time, but with a pronounced oscillatory behavior. Note that $|\lambda_1 - \lambda_2|$ separation is much smaller than the $|\lambda_3 - \lambda_4|$ separation, indicating that the space-time first approaches Type II before settling to Type D. In Fig. 7 we plot the values of the pairs (λ_1, λ_2) and (λ_3, λ_4) on the complex plane at the point $(5, 0, 0)$ for times $t = 57, \dots, 166.25$ in steps of 0.59375 . From the plots we can see how each of the two roots in the root pairs approach each other. In Fig. 4 we plot the magnitude of the root separations normalized by the difference between the average value of the roots in each pair. It takes about $80M$ of evolution, or $65M$ post

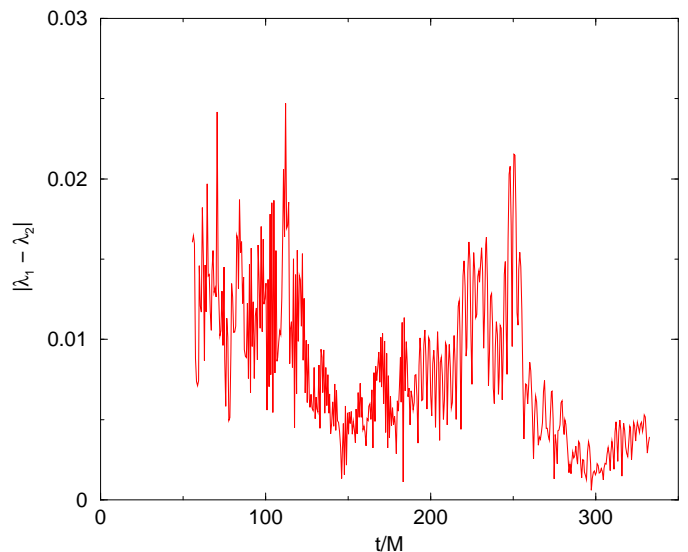


FIG. 2: The magnitude of the root-pair separation $|\lambda_1 - \lambda_2|$ versus time for the two roots close to $\lambda = 0$ at the point $x = 5M, y = 0, z = 0$.

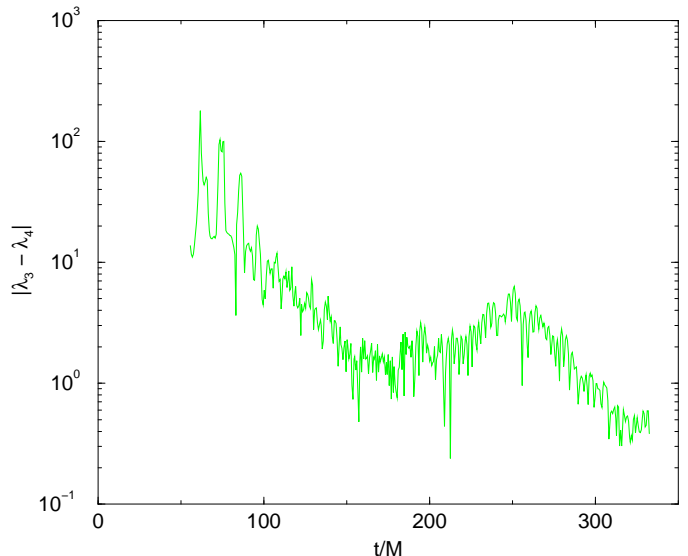


FIG. 3: The magnitude of the root-pair separation $|\lambda_3 - \lambda_4|$ versus time for the two roots furthest from $\lambda = 0$ at the point $x = 5M, y = 0, z = 0$.

merger, until the larger normalized root separation falls below 1.

In Fig. 8 we plot the function $r\Im(I)/\Re(I)$ along the x -axis for various times from $t \sim 100$ to $t \sim 350M$. It is clear from the plot that this function does not tend to ∞ at larger r , which indicates that the NUT charge of the space time vanishes. Hence we can see good evidence that the spacetime is approaching Type D with zero NUT charge, and hence is approaching a Kerr spacetime. In addition, one can, in principle, determine the a parameter (specific spin) of the remnant from the

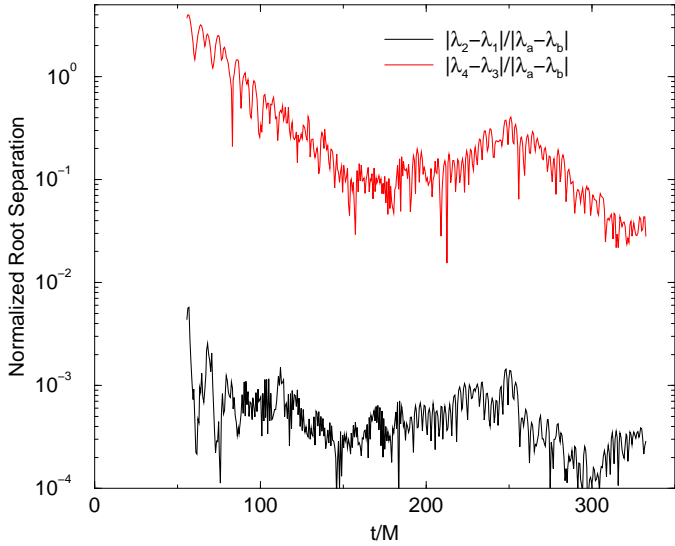


FIG. 4: The magnitude of the two root-pair separations normalized by the magnitude of the differences of the average value of the roots in each pair $|\lambda_a - \lambda_b|$, where $\lambda_a = (\lambda_1 + \lambda_2)/2$ and $\lambda_b = (\lambda_3 + \lambda_4)/2$.

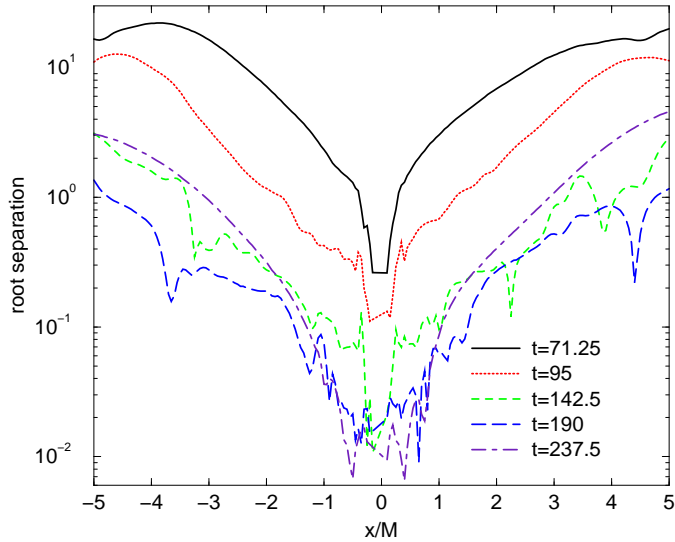


FIG. 5: The magnitude of the root-pair separation $|\lambda_3 - \lambda_4|$ along the x -axis for several values of t .

asymptotic behavior of $\Im(I)/\Re(I)$ through Eq. (29) (i.e. $\Im(I)/\Re(I) \sim 6a \cos(\theta)/r + \mathcal{O}(r^{-2})$). From the spin magnitude and direction of the remnant, we have $6a \cos(\theta) = 0.0097 \pm 0.0002$ on the x -axis, which we can reproduce to within a factor of 2 through a fit of the data in Fig. 8 to the asymptotic form $\Im(I)/\Re(I) \sim a/r + b/r^2 + c/r^2$. We have confirmed that the constraints converge to zero for our code outside of the horizons. For this simulation the constraint violations were of order 10^{-4} at the horizons, and dropped off steeply with radius. Convergence of the constraints is important to show that the space-

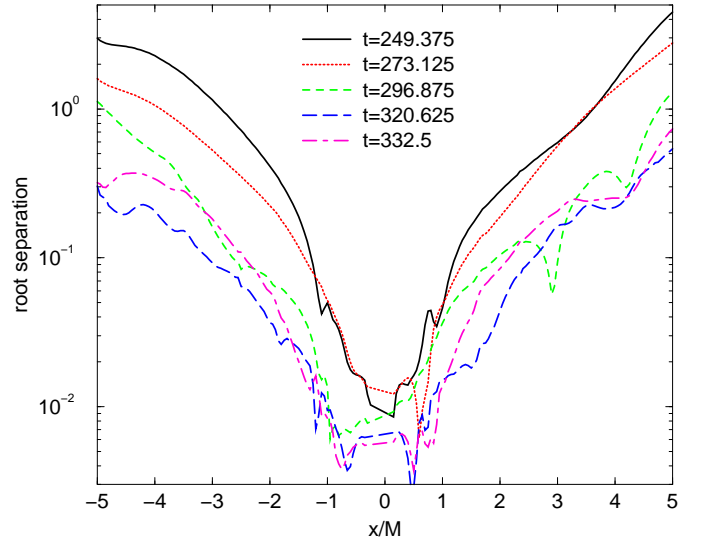


FIG. 6: The magnitude of the root-pair separation $|\lambda_3 - \lambda_4|$ along the x -axis for several values of t .

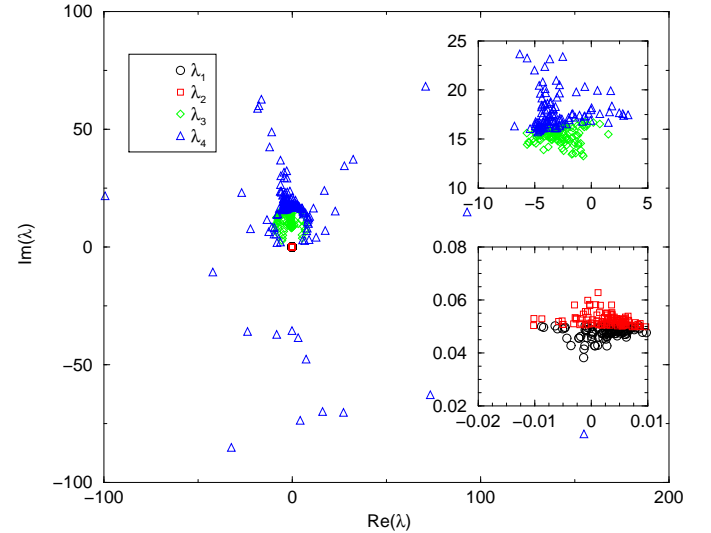


FIG. 7: The locations on the complex plane of the roots $\lambda_1, \dots, \lambda_4$ for $t = 57, 57.59375, \dots, 166.25$ at the point $(x = 5, y = 0, z = 0)$. The insets show the last 107 points. Note that λ_4 has the largest scatter in time and that the separation of λ_1 and λ_2 is not distinguishable on the overall plot.

time remains a vacuum spacetime outside of the remnant horizons (otherwise proving that the spacetime is Type D would not imply that it is Kerr).

V. CONCLUSION

We have provided a method to classify numerically generated spacetimes according to their algebraic properties. This is based on the use of the coincidence of the principal null directions for algebraically special space-

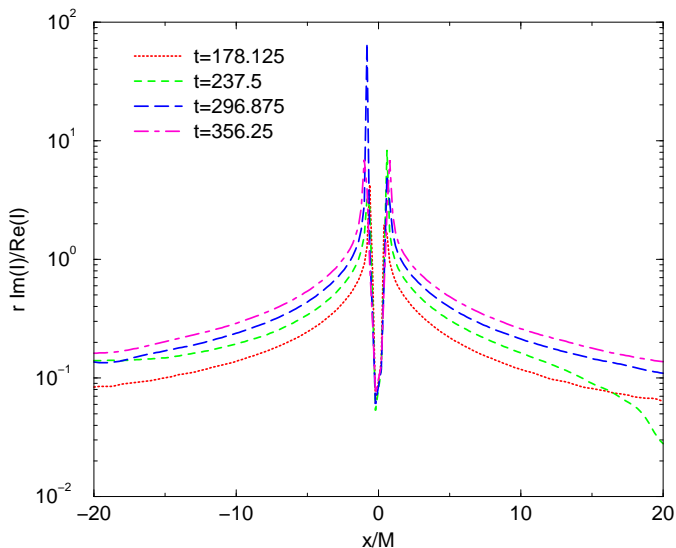


FIG. 8: The ratio $r\Im(I)/\Re(I)$ as a function of x along the x -axis. Note that the behavior indicates that $\Im(I)/\Re(I) \rightarrow 0$ as $r \rightarrow \infty$, which indicates that the NUT charge vanishes.

times. In particular, we focus on the final remnant of a generic-black-hole-binary merger, that, according to the ‘no hair’ theorem, is expected to produce a Kerr black hole, and hence be of algebraic (Petrov) type D (i.e. that the four principal null directions agree in pairs). We give a measure of the agreement by normalizing the numerical differences between two nearby roots of Eq. (3) with the average separation to the other root pair in the complex plane.

We have been able to verify this agreement to order 10^{-4} and 10^{-2} for the two pairs respectively. We find that the agreement of the two roots in each pair improves

with evolution time and only appears to be limited by unphysical boundary effects (from the refinement and outer boundaries). The late-time behavior of these two root pairs implies that the spacetime near the remnant first approaches a type II (with one pair of roots and two distinct roots) and over longer timescales approaches type D. Thus, our simulations would suggest that the space-time indeed approaches Kerr, which incidentally, is also a strong test of the stability of the Kerr solution under large, generic perturbations within the timescales of the simulation.

These results represent the first such tests for generic binary mergers using modest computational resources. This naturally suggests that further studies, perhaps also involving other numerical evolution methods, such as Pseudo-spectral [90, 91] and multi-patch, multi-block [92, 93], be used to test the algebraic structure of the remnants of binary mergers. Finally, the algebraic structure of the remnants from the merger of more than two black holes (e.g. close-encounters [56, 57] of multiple black holes), while expected to have the same structure as the remnants of binaries, could conceivably have different algebraic structures. Thus it would be interesting to use these techniques to examine those remnants.

Acknowledgments

We thank S.Dain and M.Mars for insightful comments. We gratefully acknowledge NSF for financial support from grant PHY-0722315, PHY-0653303, PHY 0714388, and PHY 0722703; and NASA for financial support from grant NASA 07-ATFP07-0158. Computational resources were provided by Lonestar cluster at TACC and by NewHorizons at RIT.

-
- [1] F. Pretorius, Phys. Rev. Lett. **95**, 121101 (2005), gr-qc/0507014.
 - [2] M. Campanelli, C. O. Lousto, P. Marronetti, and Y. Zlochower, Phys. Rev. Lett. **96**, 111101 (2006), gr-qc/0511048.
 - [3] J. G. Baker, J. Centrella, D.-I. Choi, M. Koppitz, and J. van Meter, Phys. Rev. Lett. **96**, 111102 (2006), gr-qc/0511103.
 - [4] M. Campanelli, C. O. Lousto, and Y. Zlochower, Phys. Rev. D **74**, 041501(R) (2006), gr-qc/0604012.
 - [5] M. Campanelli, C. O. Lousto, and Y. Zlochower, Phys. Rev. D **74**, 084023 (2006), astro-ph/0608275.
 - [6] M. Campanelli, C. O. Lousto, Y. Zlochower, B. Krishnan, and D. Merritt, Phys. Rev. **D75**, 064030 (2007), gr-qc/0612076.
 - [7] M. Campanelli, C. O. Lousto, and Y. Zlochower, Phys. Rev. D **73**, 061501(R) (2006).
 - [8] B. Bruggmann et al., Phys. Rev. **D77**, 024027 (2008), gr-qc/0610128.
 - [9] J. G. Baker, J. Centrella, D.-I. Choi, M. Koppitz, and J. van Meter, Phys. Rev. D **73**, 104002 (2006), gr-qc/0602026.
 - [10] F. Pretorius, Class. Quant. Grav. **23**, S529 (2006), gr-qc/0602115.
 - [11] F. Pretorius and D. Khurana, Class. Quant. Grav. **24**, S83 (2007), gr-qc/0702084.
 - [12] J. G. Baker, J. R. van Meter, S. T. McWilliams, J. Centrella, and B. J. Kelly, Phys. Rev. Lett. **99**, 181101 (2007), gr-qc/0612024.
 - [13] A. Buonanno, G. B. Cook, and F. Pretorius, Phys. Rev. **D75**, 124018 (2007), gr-qc/0610122.
 - [14] J. G. Baker et al., Phys. Rev. **D75**, 124024 (2007), gr-qc/0612117.
 - [15] M. A. Scheel et al., Phys. Rev. **D74**, 104006 (2006), gr-qc/0607056.
 - [16] J. G. Baker, M. Campanelli, F. Pretorius, and Y. Zlochower, Class. Quant. Grav. **24**, S25 (2007), gr-qc/0701016.
 - [17] P. Marronetti et al., Class. Quant. Grav. **24**, S43 (2007), gr-qc/0701123.

- [18] H. P. Pfeiffer et al., *Class. Quant. Grav.* **24**, S59 (2007), gr-qc/0702106.
- [19] U. Sperhake, V. Cardoso, F. Pretorius, E. Berti, and J. A. Gonzalez (2008), 0806.1738.
- [20] M. Campanelli, C. O. Lousto, Y. Zlochower, and D. Merritt, *Astrophys. J.* **659**, L5 (2007), gr-qc/0701164.
- [21] M. Campanelli, C. O. Lousto, Y. Zlochower, and D. Merritt, *Phys. Rev. Lett.* **98**, 231102 (2007), gr-qc/0702133.
- [22] B. Krishnan, C. O. Lousto, and Y. Zlochower, *Phys. Rev. D* **76**, 081501 (2007), arXiv:0707.0876 [gr-qc].
- [23] S. Dain, C. O. Lousto, and Y. Zlochower, *Phys. Rev. D* **78**, 024039 (2008), 0803.0351.
- [24] M. Campanelli, *Class. Quant. Grav.* **22**, S387 (2005), astro-ph/0411744.
- [25] F. Herrmann, D. Shoemaker, and P. Laguna, *AIP Conf.* **873**, 89 (2006), gr-qc/0601026.
- [26] J. G. Baker et al., *Astrophys. J.* **653**, L93 (2006), astro-ph/0603204.
- [27] C. F. Sopuerta, N. Yunes, and P. Laguna, *Phys. Rev. D* **74**, 124010 (2006), astro-ph/0608600.
- [28] J. A. González, U. Sperhake, B. Bruggmann, M. Hannam, and S. Husa, *Phys. Rev. Lett.* **98**, 091101 (2007), gr-qc/0610154.
- [29] C. F. Sopuerta, N. Yunes, and P. Laguna, *Astrophys. J.* **656**, L9 (2007), astro-ph/0611110.
- [30] F. Herrmann, I. Hinder, D. Shoemaker, and P. Laguna, *AIP Conf. Proc.* **873**, 89 (2006).
- [31] F. Herrmann, I. Hinder, D. Shoemaker, and P. Laguna, *Class. Quant. Grav.* **24**, S33 (2007).
- [32] F. Herrmann, I. Hinder, D. Shoemaker, P. Laguna, and R. A. Matzner, *Astrophys. J.* **661**, 430 (2007), gr-qc/0701143.
- [33] M. Koppitz et al., *Phys. Rev. Lett.* **99**, 041102 (2007), gr-qc/0701163.
- [34] D.-I. Choi et al., *Phys. Rev. D* **76**, 104026 (2007), gr-qc/0702016.
- [35] J. A. González, M. D. Hannam, U. Sperhake, B. Bruggmann, and S. Husa, *Phys. Rev. Lett.* **98**, 231101 (2007), gr-qc/0702052.
- [36] J. G. Baker et al., *Astrophys. J.* **668**, 1140 (2007), astro-ph/0702390.
- [37] E. Berti et al., *Phys. Rev. D* **76**, 064034 (2007), gr-qc/0703053.
- [38] W. Tichy and P. Marronetti, *Phys. Rev. D* **76**, 061502 (2007), gr-qc/0703075.
- [39] F. Herrmann, I. Hinder, D. M. Shoemaker, P. Laguna, and R. A. Matzner, *Phys. Rev. D* **76**, 084032 (2007), arXiv:0706.2541 [gr-qc].
- [40] B. Bruggmann, J. A. Gonzalez, M. Hannam, S. Husa, and U. Sperhake, *Phys. Rev. D* **77**, 124047 (2008), 0707.0135.
- [41] J. D. Schnittman et al., *Phys. Rev. D* **77**, 044031 (2008), 0707.0301.
- [42] K. Holley-Bockelmann, K. Gultekin, D. Shoemaker, and N. Yunes (0700), arXiv:0707.1334 [astro-ph].
- [43] D. Pollney et al., *Phys. Rev. D* **76**, 124002 (2007), arXiv:0707.2559 [gr-qc].
- [44] I. H. Redmount and M. J. Rees, *Comments on Astrophysics* **14**, 165 (1989).
- [45] D. Merritt, M. Milosavljevic, M. Favata, S. A. Hughes, and D. E. Holz, *Astrophys. J.* **607**, L9 (2004), astro-ph/0402057.
- [46] A. Gualandris and D. Merritt (2007), arXiv:0708.0771 [astro-ph].
- [47] R. C. Kapoor, *Pramana* **7**, 334 (1976).
- [48] T. Bogdanovic, C. S. Reynolds, and M. C. Miller (2007), astro-ph/0703054.
- [49] A. Loeb, *Phys. Rev. Lett.* **99**, 041103 (2007), astro-ph/0703722.
- [50] E. W. Bonning, G. A. Shields, and S. Salviander (2007), arXiv:0705.4263 [astro-ph].
- [51] S. Komossa, H. Zhou, and H. Lu, *Astrop. J. Letters* **678**, L81 (2008), 0804.4585.
- [52] S. Komossa and D. Merritt (2008), 0807.0223.
- [53] G. A. Shields, E. W. Bonning, and S. Salviander (2008), 0810.2563.
- [54] L. Rezzolla et al., *Astrophys. J.* **674**, L29 (2008), arXiv:0710.3345 [gr-qc].
- [55] U. Sperhake et al. (2007), arXiv:0710.3823 [gr-qc].
- [56] C. O. Lousto and Y. Zlochower, *Phys. Rev. D* **77**, 024034 (2008), arXiv:0711.1165 [gr-qc].
- [57] M. Campanelli, C. O. Lousto, and Y. Zlochower, *Phys. Rev. D* **77**, 101501(R) (2008), 0710.0879.
- [58] P. O. Mazur (2000), hep-th/0101012.
- [59] M. Campanelli, B. Kelly, and C. O. Lousto, *Phys. Rev. D* **73**, 064005 (2006), gr-qc/0510122.
- [60] J. Baker, M. Campanelli, and C. O. Lousto, *Phys. Rev. D* **65**, 044001 (2002), gr-qc/0104063.
- [61] J. Baker and M. Campanelli, *Phys. Rev. D* **62**, 127501 (2000).
- [62] O. Dreyer, B. Krishnan, D. Shoemaker, and E. Schnetter, *Phys. Rev. D* **67**, 024018 (2003), gr-qc/0206008.
- [63] M. Campanelli and C. O. Lousto, *Phys. Rev. D* **59**, 124022 (1999), gr-qc/9811019.
- [64] C. O. Lousto and Y. Zlochower, *Phys. Rev. D* **76**, 041502(R) (2007), gr-qc/0703061.
- [65] M. Mars, *Class. Quant. Grav.* **16**, 2507 (1999), gr-qc/9904070.
- [66] M. Mars, *Class. Quant. Grav.* **17**, 3353 (2000), gr-qc/0004018.
- [67] B. F. Whiting, *J. Math. Phys.* **30**, 1301 (1989).
- [68] G. Dotti, R. J. Gleiser, I. F. Ranea-Sandoval, and H. Vucetich (2008), 0805.4306.
- [69] H. Stephani, D. Kramer, M. MacCallum, C. Hoenselaers, and E. Herlt, *Exact solutions to Einstein's field equations* (Cambridge, UK: Univ. Pr., 2003), 2nd Edition. 701 P.
- [70] R. A. d'Inverno and R. A. Russel-Clark, *J. Math. Phys.* **12**, 1258 (1971).
- [71] J. Carminati and R. McLenaghan, *J. Math. Phys.* **32**, 3135 (1991).
- [72] L. Gunnarsen, H. Shinkai, and K. Maeda, *Class. Quantum Grav.* **12**, 133 (1995), gr-qc/9406003.
- [73] S. Chandrasekhar, *The Mathematical Theory of Black Holes* (Oxford University Press, Oxford, England, 1983).
- [74] M. Abramowitz and I. Stegun, *Handbook of Mathematical Functions* (Dover, New York, 1972), 10th ed.
- [75] H. Stephani and E. . Steward, *J.* (2004), 3rd Edition. 396 P.
- [76] C. Beetle, M. Bruni, L. M. Burko, and A. Nerozzi, *Phys. Rev. D* **72**, 024013 (2005), gr-qc/0407012.
- [77] S. Brandt and B. Brügmann, *Phys. Rev. Lett.* **78**, 3606 (1997), gr-qc/9703066.
- [78] M. Ansorg, B. Brügmann, and W. Tichy, *Phys. Rev. D* **70**, 064011 (2004), gr-qc/0404056.
- [79] Y. Zlochower, J. G. Baker, M. Campanelli, and C. O. Lousto, *Phys. Rev. D* **72**, 024021 (2005), gr-qc/0505055.
- [80] T. Nakamura, K. Oohara, and Y. Kojima, *Prog. Theor. Phys. Suppl.* **90**, 1 (1987).
- [81] M. Shibata and T. Nakamura, *Phys. Rev. D* **52**, 5428

- (1995).
- [82] T. W. Baumgarte and S. L. Shapiro, Phys. Rev. D **59**, 024007 (1999), gr-qc/9810065.
 - [83] P. Marronetti, W. Tichy, B. Brügmann, J. Gonzalez, and U. Sperhake, Phys. Rev. **D77**, 064010 (2008), 0709.2160.
 - [84] E. Schnetter, S. H. Hawley, and I. Hawke, Class. Quantum Grav. **21**, 1465 (2004), gr-qc/0310042.
 - [85] M. Alcubierre, B. Brügmann, P. Diener, M. Koppitz, D. Pollney, E. Seidel, and R. Takahashi, Phys. Rev. D **67**, 084023 (2003), gr-qc/0206072.
 - [86] C. Gundlach and J. M. Martin-Garcia, Phys. Rev. **D74**, 024016 (2006), gr-qc/0604035.
 - [87] J. Thornburg, Class. Quantum Grav. **21**, 743 (2004), gr-qc/0306056.
 - [88] M. Campanelli, C. O. Lousto, H. Nakano, and Y. Zlochower (2008), 0808.0713.
 - [89] F. Echeverría, Phys. Rev. D **40**, 3194 (1989).
 - [90] M. Boyle, L. Lindblom, H. Pfeiffer, M. Scheel, and L. E. Kidder, Phys. Rev. **D75**, 024006 (2007), gr-qc/0609047.
 - [91] M. Tiglio, L. E. Kidder, and S. A. Teukolsky, Class. Quant. Grav. **25**, 105022 (2008), 0712.2472.
 - [92] E. Schnetter, P. Diener, E. N. Dorband, and M. Tiglio, Class. Quant. Grav. **23**, S553 (2006), gr-qc/0602104.
 - [93] B. Zink, E. Schnetter, and M. Tiglio, Phys. Rev. **D77**, 103015 (2008), 0712.0353.